Price of Anarchy for Green Digital Twin Enabled Logistics

Manuele Favero, Chiara Schiavo, Alessandro Buratto and Leonardo Badia
Dept. of Information Engineering, University of Padova, via Gradenigo 6/b, 35131 Padua, Italy
Emails: {faveromanu,schiavochi,burattoale,badia}@dei.unipd.it

***Abstract*—In the era of smart cities and Industry 4.0, Digital Twin (DT) technologies have emerged as transformative tools for optimizing urban and industrial systems. We explore the application of Green DTs (GDTs) in the context of Third-Party Logistics (3PL) to enhance sustainability and operational efficiency. By integrating real-time data with predictive analytics, GDTs enable the optimization of delivery networks, minimizing resource consumption and carbon emissions, while addressing challenges such as traffic congestion and reverse logistics. We investigate a 3PL scenario, involving a large-scale delivery network, focusing on the misalignment between environmental goals of the central operator and the profit-driven strategies of third party providers. We employ a game-theoretic approach to evaluate inefficiencies through the Price of Anarchy (PoA) and the Price of Stability (PoS). The results demonstrate the potential of GDTs to dynamically model agent behavior, optimize route planning, and enhance collaboration in decentralized supply chain networks to reduce emissions.**

***Index Terms*—Price of Anarchy, Digital Twins, Sustainability, Logistics, Supply Chain, Game theory.**

I. Introduction

In recent years, smart cities have gained prominence as a promising solution to global challenges such as climate change and resource depletion. Governments and industries have accelerated the deployment of sensors and IoT technologies in urban environments, enabling the collection of real-time data to enhance decision-making and operational efficiency [1], [2]. This trend has catalyzed the adoption of Digital Twin (DT) technologies, to create virtual replicas of physical systems, even entire cities [3], providing a platform for optimizing resource management in urban contexts [4].

Within logistics, DTs have been tailored to address challenges in supply chain management, including minimizing pollution, as well as promoting sustainable practices and process optimization by integrating real-time monitoring and predictive capabilities [5], [6].

A significant evolution in this field is the emergence of Green Digital Twins (GDTs), which focus explicitly on sustainability goals. GDTs integrate real-time data with predictive analytics to optimize energy use, reduce emissions, and support carbon neutrality [7], [8]. They are instrumental in logistics, as enablers of comprehensive emission mapping, and supporting reverse logistics strategies to reduce environmental impact [9]. Additionally, GDTs offer tools for forecasting and managing road freight emissions, aligning logistics with global sustainability goals [10], e.g. through carbon trading mechanisms that involve the use of a marketplace to buy and sell credits that allow companies or other parties to emit a certain amount of carbon dioxide [11], [12].

This work has been supported by the Italian PRIN project 2022PNRR "DIGIT4CIRCLE," project code P2022788KK.

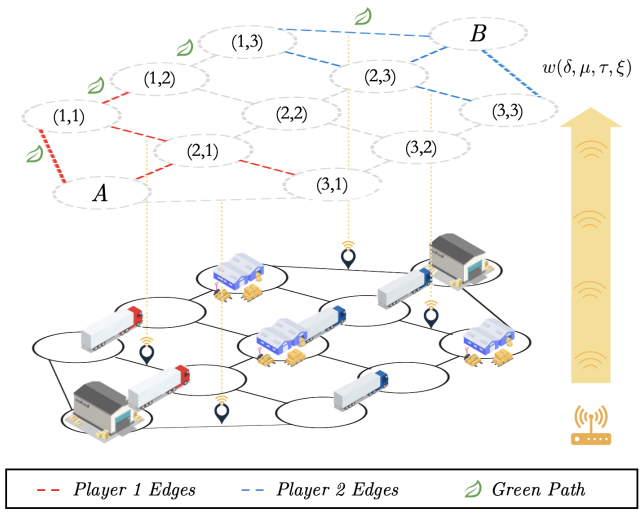

Fig. 1. Interplay between a Digital Twin framework and a GDT applied to a multi-node Third-Party Logistics 3PL network.

DTs may be extremely beneficial in the context of Third-Party Logistics (3PL), where activities such as transportation, warehousing, and distribution are outsourced to specialized providers [13]. Modern 3PL systems can leverage the real-time insights provided by DTs, which help manage complex dynamic processes across multiple locations, reduce maintenance costs, and adapt to fluctuating demands [14].

We analyze a 3PL transportation network managed by a large company overseeing numerous routes directly while outsourcing segments to third-party operators. The company aims to minimize environmental impact by determining optimal routes using a weighted shortest-path approach. However, third-party operators, motivated by profit maximization, may deviate from globally optimal solutions, introducing inefficiencies. The GDT system is leveraged to predict and analyze this scenario within a game theory framework.

Fig. 1 shows the GDT system, with the physical transportation network of warehouses and trucks displayed in the lower layer, while the upper layer illustrates the virtual DT model,

representing nodes and edges optimized for environmental and operational metrics. Edge weights $w_i(\delta, \mu, \tau, \xi)$ encode dynamic factors such as emissions, travel time, and cost, enabling real-time optimization and coordination between stakeholders. By simulating agent behavior and identifying stable working points, the DT offers a dynamic, scalable, and cost-effective alternative to traditional approaches, reducing operational overhead and enhancing decision-making.

Game-theorethic investigations to green logistic management are less explored in the literature, with few exceptions [15], [16]. Moreover, GDTs are applied to logistics with the aim to find the optimal solution for a certain task [17]. Differently from those papers, our contribution lies in leveraging game theory for 3PL settings, where third-party providers manage segments of the logistics network. Instead of just seeking optimal solutions, we focus on identifying equilibria that realistically capture decision-making dynamics.

The system's efficiency is quantified using Price of Anarchy (PoA) and Price of Stability (PoS), so as to evaluate whether self-interested behavior deviates from the most environmentally sustainable solution [18]. The main finding is that the PoA may be subject to spikes, especially in the case of low rewarding deliveries, whereas the PoS is relatively limited. This suggests that a careful equilibrium selection mechanism is required to drive the system toward efficient allocations even under de-centralized management [19].

The remainder of this paper is organized as follows: in section II, we describe our system model, outlining in subsection II-A the synthetic topology and in subsection II-B the real-world dataset used to validate the obtained results. In section III, we analyze the presented scenario from a game-theoretic perspective, introducing the algorithm employed for the simulations. In Section IV, we describe the obtained results, while in Section V we conclude.

II. System Model

In this section, we first model our scenario providing the mathematical formulation for network topology and describe how we quantify the environmental impact. In II-A, we introduce our synthetic topology and in II-B, we explain how we collect real-world data to develop the model.

A transportation logistics system is represented as a GDT, modeled as a directed, connected, and without self-loops graph $\mathcal{G}{=}(\mathcal{V}, \mathcal{E}, \mathcal{W})$. This formulation enables simulating the network dynamics and decision-making processes. Nodes $v_1, \ldots, v_n \in \mathcal{V}$ represent loading and unloading hubs within the supply chain, while edges $e_1, \ldots, e_m \in \mathcal{E}$ correspond to the roads connecting these hubs. Each edge is associated with a weight $w_1(\delta, \mu, \tau, \xi), \ldots, w_m(\delta, \mu, \tau, \xi) \in \mathcal{W}$, where $w_i(\delta, \mu, \tau, \xi) \subseteq [0, 1]$. We leverage GDT collected parameters, which impact energy consumption and emissions, to calculate the Carbon Footprint (CF) and we apply it for the edge weights. CF is the total amount of greenhouse gas emissions, primarily carbon dioxide (CO_2), generated directly or indirectly by an activity, process, or entity. In the context of logistics, it encompasses emissions resulting from transportation, warehousing, and energy consumption throughout the supply chain [20]. Therefore, weight w can be viewed as a function that approximates CF along a specific edge and it can be expressed in terms of a CF model represented as $\mathcal{F}(\delta, \mu, \tau, \xi)$, i.e.,

$$w(\delta, \mu, \tau, \xi) = \mathcal{F}(\delta, \mu, \tau, \xi). \tag{1}$$

The CF is calculated as $\mathrm{kgCO_2}$ as defined by [21]

$$\mathcal{F}_{(\mathrm{kgCO_2})} = \tau \cdot \xi \cdot 10^{-6} \cdot \sum_{i=P} (\delta_i \cdot \mu_i) \tag{2}$$

where δ_i is the distance traveled in the considered segment. Value τ is defined as

$$\tau = \frac{t_{avg}}{t_{ideal}} \tag{3}$$

and represents the traffic coefficient, defined as the ratio between the actual average travel time on a route and the ideal travel time. Conversely ξ is the emission coefficient depending on the fuel used, i.e.

$$\xi = CKB \tag{4}$$

where C is the potential carbon emission factor, K is the carbon conversion factor and B is the carbon oxidation rate [21]. The vehicle efficiency coefficient μ_h is influenced by the forces F_h acting along the path. The set of possible street categories is defined as $h \in \{\text{flat, uphill, downhill}\}$.

$$\mu_h = \frac{F_h}{n_{tf} n_m} \tag{5}$$

In (5), n_{tf} represents the transmission efficiency, accounting for mechanical losses, while n_m denotes the fuel utilization rate of the engine [21].

We calculated the emissions for each road segment, represented as edges in the graph, and assigned the corresponding CF values as edge weights in our logistics network. The network is primarily managed by a large company that controls a subset of proprietary hubs and routes, which are always active. Outsourced companies manage specific routes and decide whether to activate them. Activating a route means assigning a driver with a vehicle ready to transport goods between two nodes. When a route is activated, the travel cost must be covered, which in our case corresponds to the edge weight, representing the estimated emissions for that route. However, some edges are not owned by the large company but are outsourced to two third-party companies, which independently decide to activate them based on operational costs and potential rewards.

The primary goal of the logistics company is to offer the minimum possible reward $\mathcal{R}$ to these operators while ensuring the shortest weighted path is used, calculated via Dijkstra's algorithm [22]. The graph weights represent the estimated CF for each route, so the shortest path in our case is the one with the lowest emissions. This approach aims to minimize pollution levels by rewarding third party companies

for activating edges with the lowest CF across the network. The third-party operators aim to maximize their profits by determining the most cost-effective strategy for activating their routes. Collaboration between these operators and the logistics company can lead to improved social welfare, reducing emission and environmental impact by pooling routes. However, the reward mechanism plays a critical role in promoting such collaboration. If the reward $\mathcal{R}$ is set too low, it may fail to cover the operational costs required to activate certain routes, discouraging the companies from participating. In extreme cases, this lack of participation could result in the inability to complete the delivery. We study the behavior of 3PL companies in this scenario using two approaches: a predefined topology with synthetic data, as described in II-A, and real-world data, as discussed in II-B.

A. Synthetic Topology

We conducted an initial analysis using a lattice with a predefined topology. The transportation system we construct ensures that goods are delivered from an origin node A to a destination node B, both considered external to a 3×3 lattice $\mathcal{G}$, as shown in Fig. 2. Thus, the graph representing the logistics network consists of $n = 11$ nodes and $m = 18$ edges in total. This lattice serves as the starting structure from which sub-graphs are generated, as detailed in Alg. 1. In the simulations, we apply dropout to edges, causing variations in both the network topology and the set of reachable nodes.

In this model, the edge weights are randomly assigned following a uniform distribution $w{\sim}\mathcal{U}[0,1]$ to ensure an unbiased baseline assignment, allowing for the assessment of model behavior and preliminary evaluation of efficiency and parties decision-making patterns.

B. Real World Data

We also conducted experiments in a real-world scenario to validate the use of GDTs for logistics. We selected 11 interconnected cities in Northern Italy, corresponding to major logistics hubs and connected by highways, to construct the topology shown in Fig. 3.

We created this scenario leveraging data by the Italian National Institute of Statistics [23], comprising up-to-date time and space distances between Italian cities, reflecting real travel conditions, as derived from the 2020 TomTom Multinet road graph. This incorporates speed profiles that account for traffic impedance, such as congestion and road barriers, at different times of the day. Calculations used the ArcGIS Network Analyst's OD Cost Matrix tool to determine the travel times and distances between municipality centroids as of January 1, 2021. The travel time between cities is computed in two ways: the first is an ideal estimation based only on the distance, while the second accounts for the average traffic conditions along the route.

Finally, we took the technical specifications of a possible vehicle for the transportation-related data (frontal area, maximum payload, aerodynamic drag coefficient). We used the data of IVECO Eurocargo [24], one of the most common

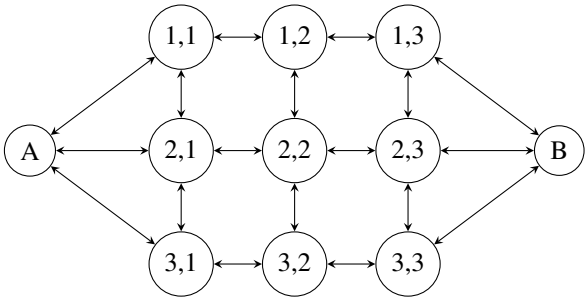

Fig. 2. Synthetic lattice topology

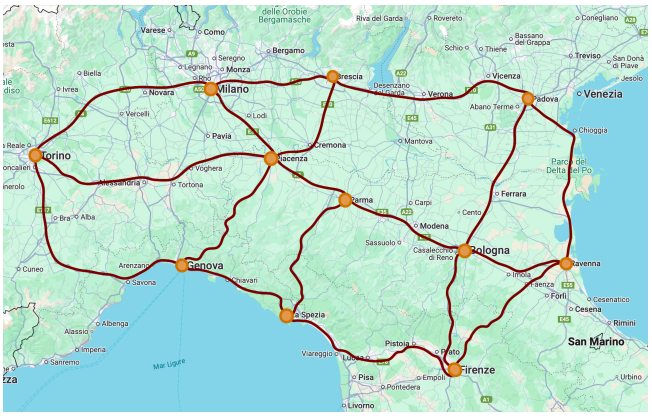

Fig. 3. Map of the cities utilized as nodes in the real scenario for logistic transport simulation.

trucks for logistics in Italy, and its consumption as fueled by gasoline type 92 to compute the CF for each path. The values were normalized with a min-max approach. Table I describes the vehicle-related variables to compute CF.

III. Game Theoretic Analysis

The scenario is modeled as a static game of complete information, where the two outsourced companies, referred to as players p_1 and p_2, must decide which road segments their transporters should activate to achieve the delivery goal.

Each player $p \in \{p_1, p_2\}$ controls a subset of edges $\mathcal{E'}_p \subset \mathcal{E}$, and their strategy involves deciding whether to activate each edge in their subset. A strategy profile, denoted $s = (s_{p_1}, s_{p_2})$, specifies the choices of both players, where $s_p \in \mathcal{S}_p$ represents the set of all possible combinations of active edges for player p. The size of the strategy space for each player is $|\mathcal{S}_p| = 2^{|\mathcal{E'}_p|}$, reflecting the binary choice for each edge. If the activated edges of both players, combined with the always-active edges owned by the large company, create a valid path between the origin A and the destination B, the goods are delivered, and the reward $\mathcal{R}$ is assigned. To discourage deviations from the weighted shortest path, the large company applies to the reward $\mathcal{R}$ the penalty deviation coefficient η_{Nash}, defined as:

$$\eta_{Nash} = \frac{d_{min}}{d_{Nash}}, \tag{6}$$

TABLE I
REAL DATA VARIABLES

Symbol	Full Name	Value	Source
C	Potential Carbon Emission Factor	18.9	[21]
K	Carbon Conversion Factor	3.67	
B	Carbon Oxidation Rate	0.98	
n_{tf}	Transmission Efficiency	0.85	
n_m	Fuel Utilization Rate of the Engine	0.27	

where d_{min} is the length of the shortest weighted path, and d_{Nash} is the length of the path resulting from the NE strategy profile. This coefficient penalizes deviations from the globally optimal path and it characterizes the efficiency of the NE referred to path selection. The utility function u_p that player p tries to maximize is:

$$u_p = \begin{cases} -\sum_{e_j \in s_p} w_j(\delta, \mu, \tau, \xi) + \eta_{Nash} \cdot \mathcal{R}, & \text{if delivered} \\ 0, & \text{otherwise} \end{cases} \tag{7}$$

where $w_j(\delta, \mu, \tau, \xi)$ is the activation cost of edge e_j.

If no valid path exists due to the absence of activated edges required to complete the route, the delivery fails, resulting in a utility function of zero for the players. This scenario is referred to as a non-cooperation case, as both players follow a selfish strategy that does not lead to task completion.

Each player p has complete knowledge of the graph and the strategies available to all players, and decides simultaneously and independently which edges to activate [25]. We compute both pure- and mixed-strategy NEs. Our focus is on how these outcomes deviate from the optimal centralized solution, where players collaboratively activate edges forming the weighted shortest path. Furthermore, we aim to evaluate how player selfishness impacts the overall system welfare, especially by increasing pollution levels.

The performance of the game-theoretic solution is evaluated using PoA or PoS. PoA quantifies the inefficiency of decentralized decision-making by measuring the worst-case ratio between an NE cost and the global optimal cost [26]:

$$\text{PoA} = \frac{\text{Cost of Social Optimum}}{\text{Cost of Worst NE}}. \tag{8}$$

Conversely, PoS captures the best-case scenario, where players achieve the most efficient NE:

$$\text{PoS} = \frac{\text{Cost of Social Optimum}}{\text{Cost of Best NE}}. \tag{9}$$

The social optimum corresponds to the best Pareto efficient outcome. This corresponds to selecting the minimum weighted path, i.e. the path with the lowest CF. By analyzing PoA and PoS, we evaluate the trade-off between centralized and decentralized decision-making. A high PoA indicates system inefficiency due to the selfish behavior of the players [26], [27]. In this case, selfishness can lead to non-delivery of goods, unequal distribution of workloads and high levels of pollution due to the player choice of travel path with high CF levels. A PoS close to 1 suggests that cooperation could lead to near-optimal outcomes.

Algorithm 1 Graph-based simulation for reward analysis

Require: $R \leftarrow$ List of rewards
Require: $N \leftarrow$ Number of simulations
for each reward $r \in R$ **do**
  for each simulation $n \in \{1, 2, \ldots, N\}$ **do**
    Create $\mathcal{G} = (\mathcal{V}, \mathcal{E}, \mathcal{W})$
    $\mathcal{W} \leftarrow \mathcal{F}(\delta, \mu, \tau, \xi)$
    $\mathcal{G} \leftarrow edge\_dropout(\mathcal{G}, 0.25)$
    $\mathcal{E'}_1, \mathcal{E'}_2 \leftarrow edge\_partition(\mathcal{G}, 0.2)$
    $\mathcal{S}_1, \mathcal{S}_2 \leftarrow strategies\_assignment(\mathcal{E'}_1, \mathcal{E'}_2)$
    $u_{1,1} \ldots u_{N,N} \leftarrow payoff\_calculation(\mathcal{S}_1, \mathcal{S}_2)$
    compute Nash equilibria and best Pareto efficient strategy for current iteration
    save data related to PoA, PoS, and η_{Nash} for this iteration
  end for
end for

For simulations, we generate random sub-networks from the same topology using Algorithm 1, which incorporates randomness and variability. At the start of each simulation, the graph $\mathcal{G}$ is modified by pruning uniformly at random 25% of its edges, and subsets of edges $\mathcal{E'}_1$ and $\mathcal{E'}_2$ are assigned to the two players. Each player selects a strategy s_i from their strategy space $\mathcal{S}_i$, aiming to maximize their utility u_i. If a path between A and B exists, the reward $\mathcal{R}$, adjusted by η_{Nash}, is assigned. This game-theoretic framework, supported by the GDT, enables the prediction of player behavior and the design of efficient reward mechanisms. To perform simulations we leverage PyGambit [28], a Python library for analyzing and solving game theory models. It interfaces with the Gambit suite, a robust platform for game theory analysis.

IV. RESULTS

In this section, we present the simulation results obtained using Algorithm 1 in both the synthetic and the real-world data scenario.

Fig. 4 illustrates the variation of PoA and PoS as the reward $\mathcal{R}$ increases. For very low values of $\mathcal{R}$, the third-party companies p_1 and p_2 are likely to opt out of collaboration, as the costs associated with completing the routes would outweigh the potential profit. In such scenarios, $d_{Nash} \to +\infty$, indicating that no valid path exists between the origin and destination, leading to failed transportation and the reward $\mathcal{R}$ not being assigned. To ensure that at least 95% of times the delivery occurs, the reward $\mathcal{R}$ must guarantee that the utility u_p for each player p in the cooperative strategy exceeds their utility in the non-cooperative case. The utility function u_p is defined in (7), and collaboration occurs if $u_p > 0$. This leads to the following condition:

$$\mathcal{R} \geq \frac{\sum_{e_j \in s_p} w_j(\delta, \mu, \tau, \xi)}{\eta_{Nash}}. \tag{10}$$

Since the edge weights w_j are normalized within $[0, 1]$, the sum $\sum_{e_j \in s_p} w_j$ is distributed over $[0, |s_p|]$, where $|s_p|$

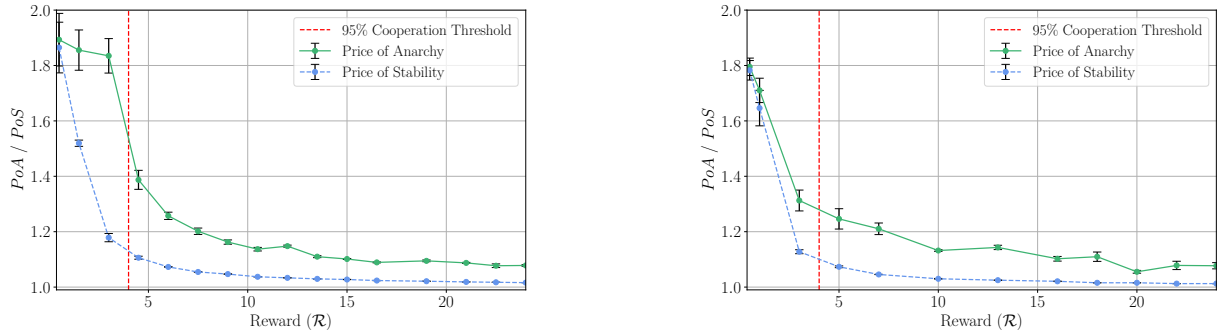

(a) Simulations (b) Real Data

Fig. 4. Variation of the Price of Anarchy and Price of Stability as a function of the reward $\mathcal{R}$. Higher rewards reduce inefficiency (PoA) and stabilize the system, with PoS converging to near-optimal levels. Error bars represent the variability across simulations.

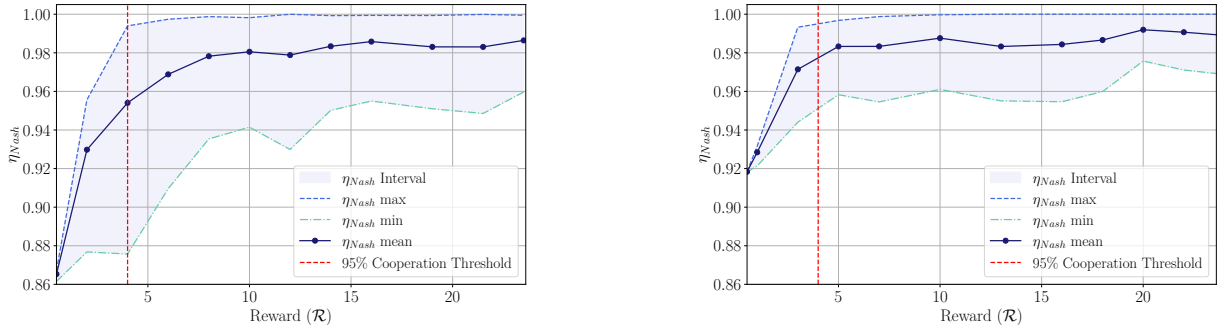

(a) Simulations (b) Real Data

Fig. 5. η_{Nash} trend versus Reward. η_{Nash} indicates how closely the emissions of the actual path align with the ideal emission levels of the minimum path calculated using Dijkstra's algorithm.

represents the number of edges in s_p. The condition for $\mathcal{R}$ can thus be rewritten as:

$$\mathcal{R} \geq \max_{p \in \{p_1, p_2\}} \frac{0.95 \cdot |s_p|}{\eta_{Nash}}. \tag{11}$$

In the given scenario, the graph initially consists of 18 edges, but each edge has a 25% probability of being removed. Remaining edges are assigned to players with a 20% probability, resulting in an expected number of edges controlled by each player of approximately $\mathbb{E}[|s_p|] \approx 3$. Assuming $\eta_{Nash} \geq 0.75$, the minimum reward required to ensure 95% collaboration is $\mathcal{R} \approx 4$. Therefore, in Fig 4 and Fig. 5 we highlight $\mathcal{R} = 4$, as the 95% cooperation threshold. The randomness introduced with Algorithm 1 influence PoA, which is sensitive to worst-case NE. To mitigate the impact of variability, we performed 50 simulations for each selected value of $\mathcal{R}$. However, for values below the threshold, collaboration often does not occur and we excluded these cases from the calculation of PoA and PoS. This results in a higher confidence interval, particularly noticeable in Fig. 4-a. Nevertheless, it is important to show the performance level achieved in these rare cases where delivery occurs.

In Fig. 4, we observe a general decreasing trend for both PoA and PoS as $\mathcal{R}$ increases. In the worst-case scenario, offering a reward lower than 4 can lead to a degradation in social welfare of over 80% compared to the social optimum. For $R < 4$, both PoA and PoS are very high, whereas, with a reward of $4 < \mathcal{R} < 5$, PoS is limited to 1.1 and although PoA remains high, it does not exceed 40% system degradation.

Further increasing the reward we achieve a minimum PoA of 1.08, representing an 8% deterioration. At the same time PoS reach its minimum at 1.02. We observe that with real data, in Fig. 4-b, PoA performance is slightly better for very low rewards. However, the overall trend remains comparable to the adopted simulations, aside from some fluctuations due to edge dropout, which is also applied in this scenario.

Fig. 5 illustrates the relationship between system efficiency, quantified by η_{Nash}, and the reward $\mathcal{R}$. We can observe how the maximum, minimum, and average η_{Nash} vary as the reward changes, always averaged over 50 iterations for each $\mathcal{R}$. As the reward increases, the system efficiency improves, reflecting players' increased alignment with optimal routing strategies. Initially, for low values of R, efficiency starts at approximately 0.91, indicating significant deviations from the optimal path. However, as $\mathcal{R}$ rises, players' strategies become more efficient, and η_{Nash} approaches a mean value of 0.99, both in simulations and real data, with

the worst NE at 0.96 and 0.97 respectively. This improvement stabilizes around $\mathcal{R} \geq 15$, where further increases in the reward yield little additional benefit.

For very low values below the cooperation threshold, the results are not satisfactory, as the minimum and maximum η_{Nash} are far from optimal, leading to problems related to equilibrium selection [19]. Conversely, for $R \geq 5$, the worst NE efficiency is above 0.9 for synthetic data and above 0.95 for real world data, with a high likelihood to get η_{Nash} very close to 1. However, with rewards below the cooperation threshold, the range is dominated by very low values, leading to significant inefficiency. Since η_{Nash} represent the deviation from the minimum weighted path, an increase in its value corresponds to a reduction in the CF and, consequently, CO_2 emissions. Specifically, for low reward values ($\mathcal{R} < 4$), emissions can increase by up to 14% in the simulations scenario (Fig. 5-a) and up to 8% in real data scenario (Fig. 5-b). However, these excess emissions decrease over time, with the worst-case scenarios showing a maximum deterioration of only 4%. These decreasing trends are a further validation for the use of GDTs in 3PL logistic scenarios.

V. Conclusions

This study highlights the potential of GDTs in 3PL systems to reduce resource consumption and carbon emissions via the integration of real-time data and predictive analytics. We quantified system inefficiencies introduced by the misalignment of environmental objectives and profit-driven strategies of 3PL operators employing a game-theoretic framework.

PoA and PoS evaluation provided insights into the trade-offs between centralized and decentralized decision-making [16]. While the PoA may be significant, the PoS is generally very low, which suggests that it is possible to achieve an efficient distributed management through proper equilibrium selection [14]. Thus, incentivizing collaboration through appropriate rewards can significantly mitigate inefficiencies and align individual strategies with global sustainability goals.

Our findings underscore the importance of using GDTs not only for dynamic route planning, but also as a tool for fostering collaboration among stakeholders in decentralized supply chains. Future research should explore the scalability of these methods in larger and more complex networks while considering additional factors such as scheduling problems [14] and DT privacy preserving [27], [29].

References

[1] O. Balaban, "Smart cities as drivers of a green economy," in *Handbook of green economics*. Elsevier, 2019, pp. 69–92.

[2] O. El Marai, T. Taleb, and J. Song, "Roads infrastructure digital twin: A step toward smarter cities realization," *IEEE Network*, vol. 35, no. 2, pp. 136–143, 2020.

[3] S. Ivanov, K. Nikolskaya, G. Radchenko, L. Sokolinsky, and M. Zymbler, "Digital twin of city: Concept overview," in *Proc. IEEE GloSIC*, 2020.

[4] T. Deng, K. Zhang, and Z.-J. M. Shen, "A systematic review of a digital twin city: A new pattern of urban governance toward smart cities," *J. Manag. Sci. Eng.*, vol. 6, no. 2, pp. 125–134, 2021.

[5] Y. Zhu, J. Cheng, Z. Liu, Q. Cheng, X. Zou, H. Xu, Y. Wang, and F. Tao, "Production logistics digital twins: research profiling, application, challenges and opportunities," *Robot. Comput.-Integr. Manuf.*, vol. 84, p. 102592, 2023.

[6] F. Benita, V. Bilò, B. Monnot, G. Piliouras, and C. Vinci, "Data-driven models of selfish routing: why price of anarchy does depend on network topology," in *Int. Conf. Web Internet Econ.*, 2020, pp. 252–265.

[7] K. Duran and B. Canberk, "Digital twin enriched green topology discovery for next generation core networks," *IEEE Trans. Green Commun. Netw.*, vol. 7, no. 4, pp. 1946–1956, 2023.

[8] F. Balduf, Z. Muller-Zhang, T. Treichel, and T. Kuhn, "Digitalizing sustainability: Product carbon footprint with green digital twins," in *Proc. IEEE ETFA*, 2024, pp. 1–8.

[9] Q. Sun, "Research on the influencing factors of reverse logistics carbon footprint under sustainable development," *Environ. Sci. Pollut. Res*, vol. 24, pp. 22 790–22 798, 2017.

[10] M. I. Piecyk and A. C. McKinnon, "Forecasting the carbon footprint of road freight transport in 2020," *Int. J. Prod. Econ.*, vol. 128, no. 1, pp. 31–42, 2010.

[11] J. Li, Q. Lu, and P. Fu, "Carbon footprint management of road freight transport under the carbon emission trading mechanism," *Math. Probl. Eng.*, vol. 2015, no. 1, p. 814527, 2015.

[12] A. McKinnon, "Green logistics: the carbon agenda," *Electron. Sci. J. Logist.*, vol. 6, no. 3, 2010.

[13] A. Calvio, F. Lenzi, A. Bujari, and L. Foschini, "Charting the route: Fine-grained road topology construction for logistics digital twins," in *Proc. IEEE Symp. Comp. Commun. (ISCC)*, 2024.

[14] S. Wu, W. Xiang, W. Li, L. Chen, and C. Wu, "Dynamic scheduling and optimization of AGV in factory logistics systems based on digital twin," *Appl. Sc.*, vol. 13, no. 3, p. 1762, 2023.

[15] M. A. Agi, S. Faramarzi-Oghani, and Ö. Hazır, "Game theory-based models in green supply chain management: a review of the literature," *Int. J. Prod. Res.*, vol. 59, no. 15, pp. 4736–4755, 2021.

[16] S. Wang and Z.-H. Hu, "Green logistics service supply chain games considering risk preference in fuzzy environments," *Sustainability*, vol. 13, no. 14, p. 8024, 2021.

[17] T. D. Moshood, G. Nawanir, S. Sorooshian, and O. Okfalisa, "Digital twins driven supply chain visibility within logistics: A new paradigm for future logistics," *Appl. Syst. Innov.*, vol. 4, no. 2, p. 29, 2021.

[18] B. Hao and C. Michini, "The price of anarchy in series-parallel network congestion games," *Math. Progr.*, vol. 203, no. 1, pp. 499–529, 2024.

[19] E. Đokanović, A. Munari, and L. Badia, "Harsanyi's equilibrium selection for distributed sources minimizing age of information," in *Proc. IEEE MedComNet*, 2024.

[20] D. Pandey, M. Agrawal, and J. S. Pandey, "Carbon footprint: current methods of estimation," *Envir. Monit. Assess.*, vol. 178, pp. 135–160, 2011.

[21] J. Xu, Y. Dong, and M. Yan, "A model for estimating passenger-car carbon emissions that accounts for uphill, downhill and flat roads," *Sustainability*, vol. 12, no. 5, p. 2028, 2020.

[22] E. W. Dijkstra, "A note on two problems in connexion with graphs," *Numerische Mathematik*, vol. 1, no. 1, pp. 269–271, 1959.

[23] ISTAT, "Distances and traveling times of italian municipalities as of 2021," accessed 31st Jan, 2025. [Online]. Available: https://www.istat.it/non-categorizzato/matrici-di-contiguita-\distanza-e-pendolarismo

[24] "IVECO eurocargo data," accessed 31st Jan, 2025. [Online]. Available: https://www.iveco.com/-/media/IVECOdotcom/SP_Content/img/ML120E18FP.pdf

[25] L. Badia, M. Levorato, F. Librino, and M. Zorzi, "Cooperation techniques for wireless systems from a networking perspective," *IEEE Wirel. Commun.*, vol. 17, no. 2, pp. 89–96, 2010.

[26] T. Roughgarden, "Selfish routing and the price of anarchy," *MIT press*, 2005.

[27] A. Buratto, A. Mora, A. Bujari, and L. Badia, "Game theoretic analysis of AoI efficiency for participatory and federated data ecosystems," in *Proc. IEEE ICC Workshops*, 2023, pp. 1301–1306.

[28] R. Savani and T. L. Turocy, "Gambit: The package for computation in game theory, version 16.3.0," *https://www.gambit-project.or*, 2025.

[29] M. Favero, T. Marchioro, and C. Schiavo, "Federated forests with differential privacy for distributed wearable sensors," in *Proc. IEEE ICARES*, 2024, pp. 1–6.